Frontiers of Information Technology & Electronic Engineering
www.jzus.zju.edu.cn; engineering.cae.cn; www.springerlink.com
ISSN 2095-9184 (print); ISSN 2095-9230 (online)
E-mail: jzus@zju.edu.cn

Stabilization of switched linear systems under asynchronous switching subject to admissible edge-dependent average dwell time*

Linlin HOU‡[1], Xuan MA[1], Haibin SUN[2]

[1]*School of Computer Science, Qufu Normal University, Rizhao 276826, China*

[2]*College of Engineering, Qufu Normal University, Rizhao 276826, China*

E-mail: houtingting8706@126.com; maxuan24@163.com; fengyun198212@163.com

Received Dec. 13, 2020; Revision accepted Mar. 7, 2021; Crosschecked Jan. 18, 2022; Published online Apr. 11, 2022

Abstract: The problem of stabilizing switched linear systems under asynchronous switching is addressed. The admissible edge-dependent average dwell time method is applied to design a switching signal that comprises slow admissible edge-dependent average dwell time and fast admissible edge-dependent average dwell time. Under this switching signal, the restriction that the maximum delay of asynchronous switching is known in advance is removed. The constructed Lyapunov function is associated with both the system mode and controller mode. The stabilization criteria and the corresponding algorithm are presented to obtain the controller gains and to design the switching signal. Finally, two examples are given to demonstrate the effectiveness of the proposed results.

Key words: Asynchronous switching; Admissible edge-dependent average dwell time; Multi-Lyapunov function
https://doi.org/10.1631/FITEE.2000698 **CLC number:** TP13

1 Introduction

In recent decades, switched systems have been widely studied due to their extensive applications in practical systems, such as power electronics systems, stirred tank reactor systems, and network control systems. Subsystems described by a collection of differential or difference equations and the switching signal that specifies the subsystem that is activated at a certain time instant together determine the behavior of a switched system (Liberzon and Morse, 1999). Surveys have shown that even if all subsystems are stable, a switched system can be unstable if the switching signal is not appropriate (Zhao et al., 2017; Li et al., 2021). However, even if all the subsystems are unstable, the switched system may be stable if the switching signal is designed reasonably (Xiang and Xiao, 2014; Lu and Yang, 2020). To date, a vast literature on stability analysis of switched systems has been presented, including Hespanha and Morse (1999), Shorten et al. (2007), Zhao et al. (2012, 2015), Zhang XL et al. (2014), Chang et al. (2020), Wang YQ et al. (2021), and Yu and Zhai (2021), to list a few.

A large number of results concerning the control synthesis of switched systems have also been reported (Deaecto et al., 2011, 2015; Yuan CZ and Wu, 2015; Zhao et al., 2016). In the abovementioned studies, switching between the subsystem and the corresponding controller is assumed to be synchronous. In fact, there is a lag between controller switching and system switching, because it takes some time to identify the system mode and apply the corresponding controller. This scenario is called "asynchronous switching" between the system

‡ Corresponding author

* Project supported by the National Natural Science Foundation of China (Nos. 61873331, 61773236, and 61773235) and the Natural Science Foundation of Shandong Province, China (No. ZR2020YQ48)

ORCID: Linlin HOU, https://orcid.org/0000-0001-7321-9239

and the controller. Asynchronous switching may decrease control performance and lead to instability. Therefore, it is necessary to study the stabilization problem of switched systems under asynchronous switching.

In the asynchronous switching scenario, the switching lag of the controller will cause the running interval of the subsystem to be divided into two parts: synchronous switching interval (SSI) and asynchronous switching interval (ASI). In SSI, the controller mode and system mode are the same, while they are different in ASI. The results in the literature indicate that the closed-loop subsystem is stable in SSI and unstable in ASI. Then, combined with the designed time-dependent switching signal, stabilization results were obtained (Zhang LX and Gao, 2010; Wang YE et al., 2013; Wang B et al., 2014). However, in fact, the unmatched controller may stabilize the corresponding subsystem in ASI, in which case, the existing results are invalid.

Many techniques have been adopted to design the time-dependent switching signal for the asynchronous switching control problem, for example, the dwell time (DT) method (Sang and Nie, 2018; Yuan S et al., 2018), average dwell time (ADT) scheme (Wang XH et al., 2016; Ren HL et al., 2018; Hua et al., 2019; Fei et al., 2020), persistent dwell time (PDT) method (Liu and Wang, 2019; Shi et al., 2019), and mode-dependent average dwell time (MDADT) method (Wang B et al., 2014; Fei et al., 2017; Wang YE et al., 2017). In these studies, the maximum asynchronous switching delay is assumed to be known a priori, and is applied to design the switching signal. However, in practice, it is difficult to determine the lag time between system switching and the switching of the corresponding controller. Hence, there is still significant research need for removing this restriction in switching signal design. The admissible edge-dependent average dwell time (AED-ADT) method has been proposed to analyze the stability of the switched systems, and to release the restrictions of MDADT switching (Hou et al., 2018a; Yang JQ et al., 2018). Can this switching signal design method be used to remove the switching signal design restriction under asynchronous switching? If so, how can it be applied? All these questions inspired us to carry out the research presented in this paper.

On the basis of the above analysis, in this paper, the problem of asynchronous switching stabilization is studied for switched linear systems. The contributions are listed as follows:

1. The switching signal is designed by combining the slow AED-ADT (SAED-ADT) method and fast AED-ADT (FAED-ADT) method, assuming that the maximum asynchronous switching delay is not known a priori.

2. The constructed Lyapunov function is associated with both the system mode and controller mode.

3. In the literature (Deaecto et al., 2011, 2015; Yuan CZ and Wu, 2015; Zhao et al., 2016), it was generally assumed that the controller cannot stabilize the subsystems in asynchronous switching intervals. In this paper, we take a different approach and investigate whether the asynchronous switching controller may be able to stabilize the subsystem in asynchronous switching intervals.

4. The stabilization criteria are obtained, and the corresponding algorithm is presented to determine the controller gains and to design the switching signal. In the simulations, two examples are provided to demonstrate the effectiveness of the proposed results.

2 Problem formulation

Consider the following switched system:

$$\dot{\boldsymbol{x}}(t)=\boldsymbol{A}_{\sigma(t)}\boldsymbol{x}(t)+\boldsymbol{B}_{\sigma(t)}\boldsymbol{u}(t), \tag{1}$$

where $\boldsymbol{x}(t)\in\mathbb{R}^n$ is the state and $\boldsymbol{u}(t)\in\mathbb{R}^p$ is the input. $\sigma(t)$, which is the switching signal, is a piecewise constant function taking its value in the finite set $\mathcal{M}=\{1,2,\dots,r\}$, where r stands for the number of subsystems. The set $\Upsilon=\{x(t_0);\ (i_0,t_0),\ (i_1,t_1),\ \dots,\ (i_m,t_m),\ \dots \mid i_m\in\mathcal{M},\ m\in\mathbb{N}\}$ is the switching sequence, where $\mathbb{N}$ is the set of natural numbers. When $t\in[t_m,t_{m+1})$, the i_m^{th} subsystem is activated. For any $i\in\mathcal{M}$, matrices $\boldsymbol{A}_i$ and $\boldsymbol{B}_i$ are supposed to be known with appropriate dimensions.

The controller is designed as

$$\boldsymbol{u}(t)=\boldsymbol{K}_{\sigma(t-d(t))}\boldsymbol{x}(t), \tag{2}$$

where $d(t)$ is the lag time satisfying $0<d(t)<t_{m+1}-t_m$, and $\boldsymbol{K}_i$ $(i\in\mathcal{M})$ is the controller gain to be determined. Substituting Eq. (2) into system (1),

we have the following closed-loop system:

$$\begin{aligned}\dot{\boldsymbol{x}}(t) &= \left(\boldsymbol{A}_{\sigma(t)} + \boldsymbol{B}_{\sigma(t)}\boldsymbol{K}_{\sigma(t-d(t))}\right)\boldsymbol{x}(t)\\ &\triangleq \boldsymbol{A}_{\sigma(t),\sigma'(t)}\boldsymbol{x}(t),\end{aligned} \tag{3}$$

where $\boldsymbol{A}_{\sigma(t),\sigma'(t)} = \boldsymbol{A}_{\sigma(t)} + \boldsymbol{B}_{\sigma(t)}\boldsymbol{K}_{\sigma(t-d(t))}$ and $\sigma'(t) = \sigma(t-d(t))$.

Remark 1 System (3) contains two classes of switching signals, i.e., $\sigma(t)$ (system mode) and $\sigma'(t)$ (controller mode). In fact, the effect of the lag time $d(t)$ is that the switching between the system and the controller is not synchronous (Fig. 1). The system switches at time instant t_m ($m \in \mathbb{N}^+$), where $\mathbb{N}^+ = \mathbb{N}/\{0\}$, and the corresponding controller switches at $t_m + d(t_m)$. Consequently, in the intervals $[t_0, t_1)$ and $[t_m + d(t_m), t_{m+1})$, the values of $\sigma(t)$ and $\sigma'(t)$ are the same. However, in $[t_m, t_m + d(t_m))$ (the shadow areas in Fig. 1), the values of these two switching signals are different. Here, the time intervals $[t_0, t_1)$ and $[t_m + d(t_m), t_{m+1})$ are called SSIs, and the time interval $[t_m, t_m + d(t_m))$ is called an ASI. Correspondingly, controller (2) is called an asynchronous switching controller.

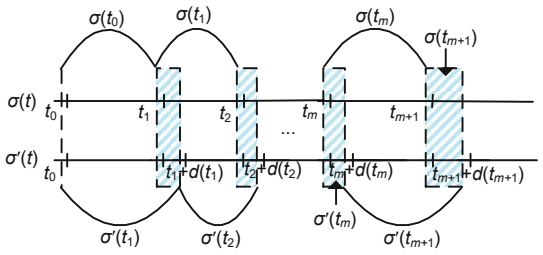

Fig. 1 Switching signals $\sigma(t)$ and $\sigma'(t)$

The following definitions will be used in the sequel.

Definition 1 (Hou et al., 2018b) For any $p, q \in \mathcal{M}$ ($p \neq q$) and $\sigma(t)$ (the switching signal), let $N^{\sigma}_{p,q}(t_1, t_2)$ be the number of switching times from q to p in the interval $[t_1, t_2)$, and $T_{p,q}(t_1, t_2)$ be the total running time of subsystem p in the interval $[t_1, t_2)$ whenever the switching takes place from q to p, where $t_2 \geq t_1 \geq 0$. In this case, $\sigma(t)$ has an SAED-ADT $\tau^{\mathrm{a}}_{p,q}$ and an FAED-ADT $d^{\mathrm{a}}_{p,q}$ if there exist nonnegative numbers $\overline{N}^0_{p,q}$ and $\underline{N}^0_{p,q}$, and positive numbers $\tau^{\mathrm{a}}_{p,q}$ and $d^{\mathrm{a}}_{p,q}$ such that the following inequalities are true:

$$N^{\sigma}_{p,q}(t_1, t_2) \leq \underline{N}^0_{p,q} + \frac{T_{p,q}(t_1, t_2)}{\tau^{\mathrm{a}}_{p,q}},\ \forall\, t_2 \geq t_1 \geq 0, \tag{4}$$

$$N^{\sigma}_{p,q}(t_1, t_2) \geq \overline{N}^0_{p,q} + \frac{T_{p,q}(t_1, t_2)}{d^{\mathrm{a}}_{p,q}},\ \forall\, t_2 \geq t_1 \geq 0, \tag{5}$$

where $\overline{N}^0_{p,q}$ and $\underline{N}^0_{p,q}$ are called the admissible edge-dependent chatter bounds.

Definition 2 (Zhao et al., 2012) The equilibrium $\boldsymbol{x} = \boldsymbol{0}$ of system (1) with $\boldsymbol{u}(t) = \boldsymbol{0}$ is globally uniformly exponentially stable (GUES) under a certain switching signal $\sigma(t)$ if there exist constants $\alpha > 0$ and $\varepsilon > 0$ such that the solution of the system satisfies $\|\boldsymbol{x}(t)\| \leq \alpha \mathrm{e}^{-\varepsilon(t-t_0)}\|\boldsymbol{x}(t_0)\|$, $\forall t \geq t_0$.

If an asynchronous switching controller (2) and an AED-ADT switching signal (containing SAED-ADT and FAED-ADT) exist such that the developed closed-loop system (3) is GUES, then switched system (1) is stabilized. In this study, the main objective is to design an asynchronous switching controller (2) and an AED-ADT switching signal such that system (1) can be stabilized.

3 Main results

In this section, we present mainly the stabilization results of system (1) under the asynchronous switching controller (2) and the designed AED-ADT switching signal.

For brevity, let t_m represent the switching instant of the subsystem and $t_m + d(t_m)$ be the switching instant of the lag controller. In the interval $[t_m, t_{m+1})$, $T_{\mathrm{s}}[t_m, t_{m+1})$ and $T_{\mathrm{u}}[t_m, t_{m+1})$ denote the SSI $[t_m + d(t_m), t_{m+1})$ and ASI $[t_m, t_m + d(t_m))$, respectively. Furthermore, let $T_{\mathrm{u}\uparrow}[t_m, t_{m+1})$ and $T_{\mathrm{u}\downarrow}[t_m, t_{m+1})$ represent the intervals in which the closed-loop subsystem is unstable and stable, respectively. For any $i, j \in \mathcal{M}$, denote $\Omega_{\mathrm{s}} = \{(i,j) \in \mathcal{M} \times \mathcal{M} | t \in T_{\mathrm{s}}[t_m, t_{m+1})\}$ and $\Omega_{\mathrm{u}} = \{(i,j) \in \mathcal{M} \times \mathcal{M} | t \in T_{\mathrm{u}}[t_m, t_{m+1})\}$. Moreover, let $\Omega_{\mathrm{u}} = \Omega_{\mathrm{u}\uparrow} \bigcup \Omega_{\mathrm{u}\downarrow}$, where $\Omega_{\mathrm{u}\uparrow} = \{(i,j) \in \mathcal{M} | t \in T_{\mathrm{u}\uparrow}[t_m, t_{m+1})\}$ and $\Omega_{\mathrm{u}\downarrow} = \{(i,j) \in \mathcal{M} | t \in T_{\mathrm{u}\downarrow}[t_m, t_{m+1})\}$.

In the sequel, we give the following result by virtue of AED-ADT switching for system (1). Suppose that subsystem j switches to subsystem i at instant t_m, and that the corresponding j^{th} controller switches to the i^{th} controller at instant $t_m + d(t_m)$.

Theorem 1 Consider system (3). For the given values $\lambda_i < 0$ ($i \in \mathcal{M}$) with $\nu_{i,j} > 1$ ($(i,j) \in \Omega_{\mathrm{s}}$), $\gamma_{i,j} < 0$ with $\mu_{i,j} > 1$ ($(i,j) \in \Omega_{\mathrm{u}\downarrow}$), and $\gamma_{i,j} > 0$ with $0 < \mu_{i,j} < 1$ ($(i,j) \in \Omega_{\mathrm{u}\uparrow}$), if there exist matrices $\boldsymbol{P}_{i,i} > 0$ ($(i,i) \in \Omega_{\mathrm{s}}$), $\boldsymbol{P}_{i,j} > 0$ ($(i,j) \in \Omega_{\mathrm{u}}$), and $\boldsymbol{K}_i$ ($i \in \mathcal{M}$) such that the following inequalities

hold:

$$(\boldsymbol{A}_i+\boldsymbol{B}_i\boldsymbol{K}_i)^{\mathrm{T}}\boldsymbol{P}_{i,i}+\boldsymbol{P}_{i,i}(\boldsymbol{A}_i+\boldsymbol{B}_i\boldsymbol{K}_i)\le\lambda_i\boldsymbol{P}_{i,i}, \quad (6)$$

$$(\boldsymbol{A}_i+\boldsymbol{B}_i\boldsymbol{K}_j)^{\mathrm{T}}\boldsymbol{P}_{i,j}+\boldsymbol{P}_{i,j}(\boldsymbol{A}_i+\boldsymbol{B}_i\boldsymbol{K}_j)\le\gamma_{i,j}\boldsymbol{P}_{i,j}, \quad (7)$$

$$\boldsymbol{P}_{i,j}\le\mu_{i,j}\boldsymbol{P}_{j,j}, \quad (8)$$

$$\boldsymbol{P}_{i,i}\le\nu_{i,j}\boldsymbol{P}_{i,j}, \quad (9)$$

then system (1) is stabilized under the asynchronous switching controller (2) and the AED-ADT switching signal satisfying

$$\begin{cases}\tau^{\mathrm{a}}_{i,j}\ge\tau^{\mathrm{a}*}_{i,j}=-\dfrac{\ln\nu_{i,j}}{\lambda_i},\ (i,j)\in\Omega_{\mathrm{s}},\\ d^{\mathrm{a}}_{i,j}\ge d^{\mathrm{a}*}_{i,j}=-\dfrac{\ln\mu_{i,j}}{\gamma_{i,j}},\ (i,j)\in\Omega_{\mathrm{u}\downarrow},\\ d^{\mathrm{a}}_{i,j}\le d^{\mathrm{a}*}_{i,j}=-\dfrac{\ln\mu_{i,j}}{\gamma_{i,j}},\ (i,j)\in\Omega_{\mathrm{u}\uparrow}.\end{cases} \quad (10)$$

Proof System (3) can be rewritten as

$$\dot{\boldsymbol{x}}(t)=\begin{cases}(\boldsymbol{A}_i+\boldsymbol{B}_i\boldsymbol{K}_i)\boldsymbol{x}(t),\ t\in T_{\mathrm{s}}[t_m,t_{m+1}),\\ (\boldsymbol{A}_i+\boldsymbol{B}_i\boldsymbol{K}_j)\boldsymbol{x}(t),\ t\in T_{\mathrm{u}}[t_m,t_{m+1}).\end{cases} \quad (11)$$

For system (11), choose the following Lyapunov function:

$$V_\varrho(\boldsymbol{x}(t))=\boldsymbol{x}^{\mathrm{T}}(t)\boldsymbol{P}_\varrho\boldsymbol{x}(t), \quad (12)$$

where $\boldsymbol{P}_\varrho>0$ and

$$\varrho=\begin{cases}(i,i), & t\in T_{\mathrm{s}}[t_m,t_{m+1}),\\ (i,j), & t\in T_{\mathrm{u}}[t_m,t_{m+1}).\end{cases}$$

When $t\in T_{\mathrm{s}}[t_m,t_{m+1})$, $\sigma(t_m)=\sigma'(t_m)=i$. Then on the basis of inequality (6), one can obtain the following inequality:

$$\begin{aligned}\dot{V}_{i,i}(t)-\lambda_iV_{i,i}(t)=\boldsymbol{x}^{\mathrm{T}}(t)\Big((\boldsymbol{A}_i+\boldsymbol{B}_i\boldsymbol{K}_i)^{\mathrm{T}}\boldsymbol{P}_{i,i}\\ +\boldsymbol{P}_{i,i}(\boldsymbol{A}_i+\boldsymbol{B}_i\boldsymbol{K}_i)-\lambda_i\boldsymbol{P}_{i,i}\Big)\boldsymbol{x}(t)\le0.\end{aligned} \quad (13)$$

Denote $\sigma(t_0)=\sigma'(t_0)=i$ when $t\in[t_0,t_1)$. Then from inequality (13), we obtain

$$V_{i,i}(t)\le\mathrm{e}^{\lambda_i(t-t_0)}V_{i,i}(t_0). \quad (14)$$

Let $\sigma(t_m+d(t_m))=\sigma'(t_m+d(t_m))=i$ when $t\in[t_m+d(t_m),t_{m+1})$. Then on the basis of inequality (13), the following inequality is true:

$$V_{i,i}(t)\le\mathrm{e}^{\lambda_i(t-(t_m+d(t_m)))}V_{i,i}(t_m+d(t_m)). \quad (15)$$

Denote $\sigma(t_m)=i,\sigma'(t_m)=j$ when $t\in[t_m,t_m+d(t_m))$. According to inequality (7), we have

$$V_{i,j}(t)\le\mathrm{e}^{\gamma_{i,j}(t-t_m)}V_{i,j}(t_m). \quad (16)$$

Note that $\sigma(t_m+d(t_m))=\sigma(t_m)$, $\sigma'(t_m+d(t_m))=\sigma'(t_{m+1})$, and $\sigma'(t_0)=\sigma'(t_1)$. When $t\in[t_m,t_m+d(t_m))$, inequalities (8), (9), and (14)–(16) mean that inequality (17) (on the top of the next page) holds.

Let $\ln\nu_{\sigma(t_0),\sigma'(t_0)}\le\ln\nu_{i,j}$. By calculation, we can obtain inequality (18) and Eq. (19) (on the top of the next page), where in the interval $[t_0,t)$, $N^\sigma_{i,j}(t_0,t)$ and $T_{i,j}(t_0,t)$ stand for the number of switching times and the total running time of the i^{th} subsystem whenever the switching occurs from subsystem j to subsystem i.

Substituting inequality (18) and Eq. (19) into inequality (17) and combining inequalities (4) and (5) yield inequality (20) (on the top of page 815).

It can be verified from Eq. (12) that

$$\begin{aligned}&\Lambda_1\le V_\varrho(\boldsymbol{x}(t))\le\Lambda_2,\\ &\Lambda_1=\min_{(i,j)\in\mathcal{M}\times\mathcal{M}}(\lambda_{\min}(\boldsymbol{P}_{i,j}))\|\boldsymbol{x}(t)\|^2,\\ &\Lambda_2=\max_{(i,j)\in\mathcal{M}\times\mathcal{M}}(\lambda_{\max}(\boldsymbol{P}_{i,j}))\|\boldsymbol{x}(t)\|^2,\end{aligned}$$

which together with inequality (20) further implies

$$\|\boldsymbol{x}(t)\|^2\le\alpha^2\mathrm{e}^{\varepsilon_{i,j}}\|\boldsymbol{x}(t_0)\|^2,$$

where

$$\begin{aligned}\alpha=&\sqrt{\frac{\max_{(i,j)\in\mathcal{M}\times\mathcal{M}}(\lambda_{\min}(\boldsymbol{P}_{i,j}))}{\min_{(i,j)\in\mathcal{M}\times\mathcal{M}}(\lambda_{\min}(\boldsymbol{P}_{i,j}))}}\\ &\times\sqrt{\exp\Bigg(\sum_{(i,j)\in\Omega_{\mathrm{s}},\,\sigma(t_l)=i}\ \sum_{\sigma'(t_l)=j}\underline{N}^0_{i,j}\ln\nu_{i,j}\Bigg)}\\ &\times\sqrt{\exp\Bigg(\sum_{(i,j)\in\Omega_{\mathrm{u}\downarrow},\,\sigma(t_l)=i}\ \sum_{\sigma'(t_l)=j}\underline{N}^0_{i,j}\ln\mu_{i,j}\Bigg)}\\ &\times\sqrt{\exp\Bigg(\sum_{(i,j)\in\Omega_{\mathrm{u}\uparrow},\,\sigma(t_l)=i}\ \sum_{\sigma'(t_l)=j}\overline{N}^0_{i,j}\ln\mu_{i,j}\Bigg)},\end{aligned}$$

$$\begin{aligned}\varepsilon_{i,j}=&\sum_{\substack{(i,j)\in\Omega_{\mathrm{s}},\\ \sigma(t_l)=i}}\ \sum_{\sigma'(t_l)=j}\Big(\frac{\ln\nu_{i,j}}{\tau^{\mathrm{a}}_{i,j}}+\lambda_i\Big)T_{i,j}(t_0,t)\\ &+\sum_{\substack{(i,j)\in\Omega_{\mathrm{u}\downarrow},\\ \sigma(t_l)=i}}\ \sum_{\sigma'(t_l)=j}\Big(\frac{\ln\mu_{i,j}}{d^{\mathrm{a}}_{i,j}}+\gamma_{i,j}\Big)T_{i,j}(t_0,t)\\ &+\sum_{\substack{(i,j)\in\Omega_{\mathrm{u}\uparrow},\\ \sigma(t_l)=i}}\ \sum_{\sigma'(t_l)=j}\Big(\frac{\ln\mu_{i,j}}{d^{\mathrm{a}}_{i,j}}+\gamma_{i,j}\Big)T_{i,j}(t_0,t).\end{aligned}$$

$$
\begin{aligned}
&V_{\sigma(t_m),\sigma'(t_m)}(t) \le \mathrm{e}^{\gamma_{\sigma(t_m),\sigma'(t_m)}(t-t_m)} V_{\sigma(t_m),\sigma'(t_m)}(t_m) \le \mathrm{e}^{\gamma_{\sigma(t_m),\sigma'(t_m)}(t-t_m)} \mu_{\sigma(t_m),\sigma'(t_m)} \\
&\cdot V_{\sigma(t_{m-1}),\sigma'(t_m)}(t_m) \le \mathrm{e}^{\gamma_{\sigma(t_m),\sigma'(t_m)}(t-t_m)} \mu_{\sigma(t_m),\sigma'(t_m)} \mathrm{e}^{\lambda_{\sigma(t_{m-1})}(t_m-(t_{m-1}+d(t_{m-1})))} \\
&\cdot V_{\sigma(t_{m-1}),\sigma'(t_m)}(t_{m-1}+d(t_{m-1})) \le \mathrm{e}^{\gamma_{\sigma(t_m),\sigma'(t_m)}(t-t_m)} \mu_{\sigma(t_m),\sigma'(t_m)} \\
&\cdot \mathrm{e}^{\lambda_{\sigma(t_{m-1})}(t_m-(t_{m-1}+d(t_{m-1})))} \nu_{\sigma(t_{m-1}),\sigma'(t_{m-1})} V_{\sigma(t_{m-1}),\sigma'(t_{m-1})}(t_{m-1}+d(t_{m-1})) \\
\le \cdots \le &\prod_{l=1}^{m} \mu_{\sigma(t_l),\sigma'(t_l)} \prod_{l=1}^{m-1} \mathrm{e}^{\gamma_{\sigma(t_l),\sigma'(t_l)} d(t_l)} \mathrm{e}^{\gamma_{\sigma(t_m),\sigma'(t_m)}(t-t_m)} \prod_{l=0}^{m-1} \nu_{\sigma(t_l),\sigma'(t_l)} \\
&\cdot \prod_{l=1}^{m-1} \mathrm{e}^{\lambda_{\sigma(t_l)}(t_{l+1}-(t_l+d(t_l)))} \mathrm{e}^{\lambda_{\sigma(t_0)}(t_1-t_0)} V_{\sigma(t_0),\sigma'(t_0)}(t_0).
\end{aligned} \tag{17}
$$

$$
\begin{aligned}
&\prod_{l=1}^{m} \mu_{\sigma(t_l),\sigma'(t_l)} \prod_{l=0}^{m-1} \nu_{\sigma(t_l),\sigma'(t_l)} = \exp\left(\sum_{l=1}^{m} \ln \mu_{\sigma(t_l),\sigma'(t_l)}\right) \exp\left(\sum_{l=0}^{m-1} \ln \nu_{\sigma(t_l),\sigma'(t_l)}\right) \\
=&\exp\left(\sum_{(i,j)\in\Omega_{\mathrm{u}}} \sum_{l=1}^{m} \sum_{\substack{\sigma(t_l)=i,\\ \sigma'(t_l)=j}} \ln \mu_{i,j}\right) \exp\left(\sum_{(i,j)\in\Omega_{\mathrm{s}}} \sum_{l=1}^{m-1} \sum_{\substack{\sigma(t_l)=i,\\ \sigma'(t_l)=j}} \ln \nu_{i,j}\right) \exp\left(\ln \nu_{\sigma(t_0),\sigma'(t_0)}\right) \\
\le&\exp\left(\sum_{\substack{(i,\,j)\,\in\,\Omega_{\mathrm{u}},\\ \sigma(t_l)\,=\,i}} \sum_{\sigma'(t_l)=j} N^{\sigma}_{i,j}(t_0,t) \ln \mu_{i,j} + \sum_{\substack{(i,\,j)\,\in\,\Omega_{\mathrm{s}},\\ \sigma(t_l)\,=\,i}} \sum_{\sigma'(t_l)=j} N^{\sigma}_{i,j}(t_0,t) \ln \nu_{i,j}\right).
\end{aligned} \tag{18}
$$

$$
\begin{aligned}
&\prod_{l=1}^{m-1} \exp\left(\gamma_{\sigma(t_l),\sigma'(t_l)}(t_{s+1}-(t_l+d(t_l)))\right) \exp\left(\gamma_{\sigma(t_m),\sigma'(t_m)}(t-t_m)\right) \prod_{l=1}^{m-1} \exp\left(\lambda_{\sigma(t_l)} d(t_l)\right) \exp\left(\lambda_{\sigma(t_0)}(t_1-t_0)\right) \\
&= \exp\left(\sum_{l=1}^{m-1} \gamma_{\sigma(t_l),\sigma'(t_l)}(t_{s+1}-(t_l+d(t_l))) + \gamma_{\sigma(t_m),\sigma'(t_m)}(t-t_m)\right) \exp\left(\sum_{l=1}^{m-1} \lambda_{\sigma(t_l)} d(t_l) + \lambda_{\sigma(t_0)}(t_1-t_0)\right) \\
&= \exp\left(\sum_{\substack{(i,\,j)\,\in\,\Omega_{\mathrm{s}},\\ \sigma(t_l)\,=\,i}} \lambda_i T_{i,j}(t_0,t) + \sum_{\substack{(i,\,j)\,\in\,\Omega_{\mathrm{u}\downarrow},\\ \sigma(t_l)\,=\,i,\\ \sigma'(t_l)\,=\,j}} \gamma_{i,j} T_{i,j}(t_0,t) + \sum_{\substack{(i,\,j)\,\in\,\Omega_{\mathrm{u}\uparrow},\\ \sigma(t_l)\,=\,i,\\ \sigma'(t_l)\,=\,j}} \gamma_{i,j} T_{i,j}(t_0,t)\right) \\
&= \exp\left(\sum_{\substack{(i,\,j)\,\in\,\Omega_{\mathrm{s}},\\ \sigma(t_l)\,=\,i}} \sum_{\sigma'(t_l)=j} \lambda_i T_{i,j}(t_0,t) + \sum_{\substack{(i,\,j)\,\in\,\Omega_{\mathrm{u}\downarrow},\\ \sigma(t_l)\,=\,i}} \sum_{\sigma'(t_l)=j} \gamma_{i,j} T_{i,j}(t_0,t) + \sum_{\substack{(i,\,j)\,\in\,\Omega_{\mathrm{u}\uparrow},\\ \sigma(t_l)\,=\,i}} \sum_{\sigma'(t_l)=j} \gamma_{i,j} T_{i,j}(t_0,t)\right).
\end{aligned} \tag{19}
$$

Let

$$
\beta = \max\left(\max_{(i,j)\in\Omega_{\mathrm{u}}}\left(\frac{\ln \mu_{i,j}}{d^{\mathrm{a}}_{i,j}} + \gamma_{i,j}\right), \max_{(i,j)\in\Omega_{\mathrm{s}}}\left(\frac{\ln \nu_{i,j}}{\tau^{\mathrm{a}}_{i,j}} + \lambda_i\right)\right).
$$

By condition (10), we can determine that $\beta < 0$. Then we have

$$
\begin{aligned}
\|\boldsymbol{x}(t)\| &\le \alpha \mathrm{e}^{\frac{1}{2}\varepsilon_{i,j}} \|\boldsymbol{x}(t_0)\| \\
&\le \alpha \mathrm{e}^{\frac{1}{2}\beta(t-t_0)} \|\boldsymbol{x}(t_0)\|.
\end{aligned} \tag{21}
$$

Moreover, the value of α is larger than 0. Then from inequality (21) and Definition 2, we conclude that system (3) is GUES, which implies that system (1) is stabilized by controller (2) and switching

$$
\begin{aligned}
V_{\sigma(t),\sigma'(t)}(t) \leq & \exp\left(\sum_{\substack{(i,j)\in\Omega_{\mathrm{s}},\\ \sigma(t_l)=i}}\sum_{\sigma'(t_l)=j}\left(N^{\sigma}_{i,j}(t_0,t)\ln\nu_{i,j}+\lambda_i T_{i,j}(t_0,t)\right)\right)\\
&\cdot\exp\left(\sum_{\substack{(i,j)\in\Omega_{\mathrm{u}\downarrow},\\ \sigma(t_l)=i}}\sum_{\sigma'(t_l)=j}\left(N^{\sigma}_{i,j}(t_0,t)\ln\mu_{i,j}+\gamma_{i,j}T_{i,j}(t_0,t)\right)\right)\\
&\cdot\exp\left(\sum_{\substack{(i,j)\in\Omega_{\mathrm{u}\uparrow},\\ \sigma(t_l)=i}}\sum_{\sigma'(t_l)=j}\left(N^{\sigma}_{i,j}(t_0,t)\ln\mu_{i,j}+\gamma_{i,j}T_{i,j}(t_0,t)\right)\right)V_{\sigma(t_0),\sigma'(t_0)}(t_0)\\
\leq & \exp\left(\sum_{\substack{(i,j)\in\Omega_{\mathrm{s}},\\ \sigma(t_l)=i}}\sum_{\sigma'(t_l)=j}\left(\left(\underline{N}^0_{i,j}+\frac{T_{i,j}(t_0,t)}{\tau^{\mathrm{a}}_{i,j}}\right)\ln\nu_{i,j}+\lambda_i T_{i,j}(t_0,t)\right)\right)\\
&\cdot\exp\left(\sum_{\substack{(i,j)\in\Omega_{\mathrm{u}\downarrow},\\ \sigma(t_l)=i}}\sum_{\sigma'(t_l)=j}\left(\left(\underline{N}^0_{i,j}+\frac{T_{i,j}(t_0,t)}{d^{\mathrm{a}}_{i,j}}\right)\ln\mu_{i,j}+\gamma_{i,j}T_{i,j}(t_0,t)\right)\right)\\
&\cdot\exp\left(\sum_{\substack{(i,j)\in\Omega_{\mathrm{u}\uparrow},\\ \sigma(t_l)=i}}\sum_{\sigma'(t_l)=j}\left(\left(\overline{N}^0_{i,j}+\frac{T_{i,j}(t_0,t)}{d^{\mathrm{a}}_{i,j}}\right)\ln\mu_{i,j}+\gamma_{i,j}T_{i,j}(t_0,t)\right)\right)V_{\sigma(t_0),\sigma'(t_0)}(t_0)\\
= & \exp\left(\sum_{\substack{(i,j)\in\Omega_{\mathrm{s}},\\ \sigma(t_l)=i}}\sum_{\sigma'(t_l)=j}\underline{N}^0_{i,j}\ln\nu_{i,j}+\sum_{\substack{(i,j)\in\Omega_{\mathrm{u}\downarrow},\\ \sigma(t_l)=i}}\sum_{\sigma'(t_l)=j}\underline{N}^0_{i,j}\ln\mu_{i,j}+\sum_{\substack{(i,j)\in\Omega_{\mathrm{u}\uparrow},\\ \sigma(t_l)=i}}\sum_{\sigma'(t_l)=j}\overline{N}^0_{i,j}\ln\mu_{i,j}\right)\\
&\cdot\exp\left(\sum_{\substack{(i,j)\in\Omega_{\mathrm{s}},\\ \sigma(t_l)=i}}\sum_{\sigma'(t_l)=j}\left(\frac{\ln\nu_{i,j}}{\tau^{\mathrm{a}}_{i,j}}+\lambda_i\right)T_{i,j}(t_0,t)\right)\exp\left(\sum_{\substack{(i,j)\in\Omega_{\mathrm{u}\downarrow},\\ \sigma(t_l)=i}}\sum_{\sigma'(t_l)=j}\left(\frac{\ln\mu_{i,j}}{d^{\mathrm{a}}_{i,j}}+\gamma_{i,j}\right)T_{i,j}(t_0,t)\right)\\
&\cdot\exp\left(\sum_{\substack{(i,j)\in\Omega_{\mathrm{u}\uparrow},\\ \sigma(t_l)=i}}\sum_{\sigma'(t_l)=j}\left(\frac{\ln\mu_{i,j}}{d^{\mathrm{a}}_{i,j}}+\gamma_{i,j}\right)T_{i,j}(t_0,t)\right)V_{\sigma(t_0),\sigma'(t_0)}(t_0).
\end{aligned}
\tag{20}
$$

signal (10). This completes the proof.

Remark 2 In Theorem 1, the stabilization condition is presented for system (1) under the asynchronous switching controller (2). Three different cases are considered to design the corresponding switching signal:

Case 1: the i^{th} subsystem is stabilized by the i^{th} controller;

Case 2: the i^{th} subsystem is stabilized by the j^{th} controller;

Case 3: the i^{th} subsystem is not stabilized by the j^{th} controller.

Case 1 means that the switching between the system and the controller is synchronous. In this case, we use SAED-ADT switching to guarantee that the dwell time is as long as possible. Cases 2 and 3 occur when the switching between the system and the controller is asynchronous. In case 2, although the activated subsystem and the controller are mismatched, $\boldsymbol{A}_i+\boldsymbol{B}_i\boldsymbol{K}_j$ is stable. Hence, SAED-ADT

switching is employed. In case 3, the mismatch between the activated subsystem and the controller may cause poor control performance, so FAED-ADT switching is used to ensure that the dwell time is as short as possible.

Remark 3 Many studies tackling the problem of asynchronous switching control for various switched systems have a premise that the maximum asynchronous switching delay is assumed to be known a priori (Wang B et al., 2014; Ren W and Xiong, 2016; Wang XH et al., 2016; Fei et al., 2017; Wang YE et al., 2017; Wu et al., 2017; Ren HL et al., 2018; Sang and Nie, 2018; Yuan S et al., 2018; Hua et al., 2019). In this study, this restriction is eliminated. By virtue of AED-ADT switching (10), the asynchronous switching delay $d^{\mathrm{a}}_{i,j}$ in every interval can be obtained, which is more in line with the demand in practice.

Remark 4 In ASIs, both the constructed multi-Lyapunov function and its decay rate are associated with the system mode and controller mode, which is more general than the one in Wang YE et al. (2013).

Remark 5 Suppose that at switching instant t_m, the j^{th} subsystem switches to the i^{th} subsystem, and that at switching instant $t_m + d(t_m)$, the j^{th} controller switches to the i^{th} controller. Then at switching instant $t_m + d(t_m)$, the energy of the Lyapunov function is allowed to increase (see the square-line area in Fig. 2). Furthermore, at switching instant t_m, the energy of the Lyapunov function is permitted to increase as long as $\boldsymbol{A}_i + \boldsymbol{B}_i\boldsymbol{K}_j$ is stable (see the slash-line area in Fig. 2a). When $\boldsymbol{A}_i + \boldsymbol{B}_i\boldsymbol{K}_j$ is not stable, the energy of the Lyapunov function must decrease at switching instant t_m (see the slash-line area in Fig. 2b). However, the increment is allowable in the ASI (see the dot-dash line in Fig. 2b).

To obtain the controller gains $\boldsymbol{K}_i$ ($i \in \mathcal{M}$), we present the following result:

Theorem 2 Consider system (3). For the given values $\lambda_i < 0$ ($i \in \mathcal{M}$) with $\nu_{i,j} > 1$ ($(i,j) \in \Omega_{\mathrm{s}}$), $\gamma_{i,j} < 0$ with $\mu_{i,j} > 1$ ($(i,j) \in \Omega_{\mathrm{u}\downarrow}$), and $\gamma_{i,j} > 0$ with $0 < \mu_{i,j} < 1$ ($(i,j) \in \Omega_{\mathrm{u}\uparrow}$), if there exist matrices $\boldsymbol{X}_{i,i} > 0$ ($(i,i) \in \Omega_{\mathrm{s}}$), $\boldsymbol{X}_{i,j} > 0$ ($(i,j) \in \Omega_{\mathrm{u}}$), and $\bar{\boldsymbol{K}}_i$ ($i \in \mathcal{M}$) such that the following inequalities hold:

$$\boldsymbol{X}_{i,i}\boldsymbol{A}_i^{\mathrm{T}} + \bar{\boldsymbol{K}}_i^{\mathrm{T}}\boldsymbol{B}_i^{\mathrm{T}} + \boldsymbol{A}_i\boldsymbol{X}_{i,i} + \boldsymbol{B}_i\bar{\boldsymbol{K}}_i \le \lambda_i\boldsymbol{X}_{i,i}, \tag{22}$$

$$\begin{aligned}\boldsymbol{X}_{i,j}\boldsymbol{A}_i^{\mathrm{T}} + \boldsymbol{A}_i\boldsymbol{X}_{i,j} + \boldsymbol{X}_{i,j}\boldsymbol{X}_{j,j}^{-1}\bar{\boldsymbol{K}}_j^{\mathrm{T}}\boldsymbol{B}_i^{\mathrm{T}} \\ + \boldsymbol{B}_i\bar{\boldsymbol{K}}_j\boldsymbol{X}_{j,j}^{-1}\boldsymbol{X}_{i,j} \le \gamma_{i,j}\boldsymbol{X}_{i,j},\end{aligned} \tag{23}$$

$$\boldsymbol{X}_{j,j} \le \mu_{i,j}\boldsymbol{X}_{i,j}, \tag{24}$$

$$\boldsymbol{X}_{i,j} \le \nu_{i,j}\boldsymbol{X}_{i,i}, \tag{25}$$

then system (1) is stabilized under the asynchronous switching controller (2) and the switching signal that satisfies condition (10). Moreover, the controller gains are given by $\boldsymbol{K}_i = \bar{\boldsymbol{K}}_i\boldsymbol{X}_{i,i}^{-1}$.

Proof On one hand, pre- and post-multiplying inequality (22) by $\boldsymbol{X}_{i,i}^{-1}$, and letting $\boldsymbol{P}_{i,i} = \boldsymbol{X}_{i,i}^{-1}$, we can obtain inequality (6). Multiplying both sides of inequality (23) by $\boldsymbol{X}_{i,j}^{-1}$, and setting $\boldsymbol{P}_{i,j} = \boldsymbol{X}_{i,j}^{-1}$, one obtains

$$\begin{aligned}-\gamma_{i,j}\boldsymbol{P}_{i,j} + \boldsymbol{A}_i^{\mathrm{T}}\boldsymbol{P}_{i,j} + \boldsymbol{P}_{i,j}\boldsymbol{A}_i + \boldsymbol{X}_{j,j}^{-1}(\boldsymbol{B}_i\bar{\boldsymbol{K}}_j)^{\mathrm{T}}\boldsymbol{P}_{i,j} \\ + \boldsymbol{P}_{i,j}\boldsymbol{B}_i\bar{\boldsymbol{K}}_j\boldsymbol{X}_{j,j}^{-1} < 0,\end{aligned} \tag{26}$$

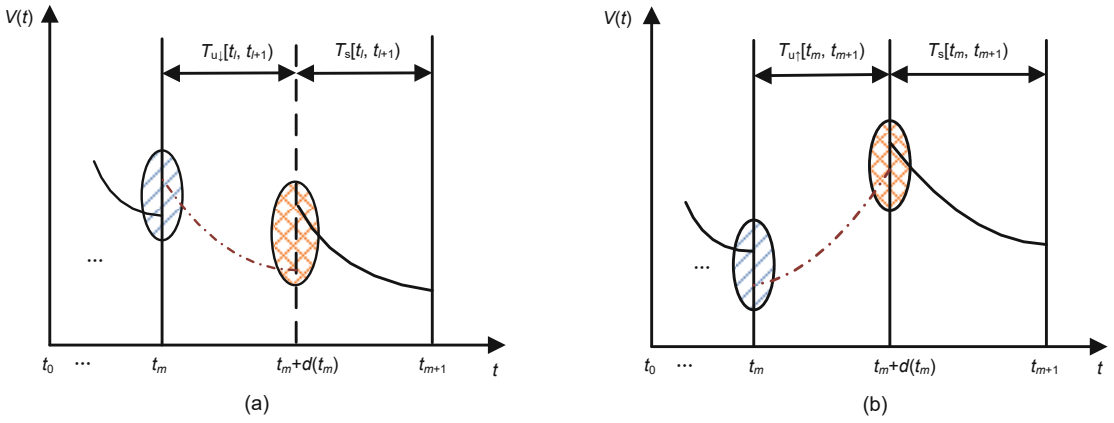

Fig. 2 Response curves of the Lyapunov function: (a) $\boldsymbol{A_i + B_iK_j}$ is stable in $[t_m, t_m + d(t_m))$; (b) $\boldsymbol{A_i + B_iK_j}$ is unstable in $[t_m, t_m + d(t_m))$

which together with $\bar{\boldsymbol{K}}_i = \boldsymbol{K}_i \boldsymbol{X}_{i,i}$ and $\boldsymbol{P}_{i,i} = \boldsymbol{X}_{i,i}^{-1}$ leads to inequality (7).

On the other hand, from inequality (24) and the Schur complement formula, we have

$$\begin{bmatrix} -\mu_{i,j}\boldsymbol{X}_{i,j} & \boldsymbol{I} \\ * & -\boldsymbol{X}_{j,j}^{-1} \end{bmatrix} \leq 0,$$

which is equivalent to $-\boldsymbol{X}_{j,j}^{-1} + (\mu_{i,j}\boldsymbol{X}_{i,j})^{-1} \leq 0$. Notice that $\boldsymbol{P}_{i,i} = \boldsymbol{X}_{i,i}^{-1}$ and $\boldsymbol{P}_{i,j} = \boldsymbol{X}_{i,j}^{-1}$, and we obtain inequality (8). In the same way, we can obtain inequality (9) from inequality (25). This completes the proof.

Note that in Theorem 2, condition (23) is nonlinear. In the following, we give an algorithm to obtain the controller gains and to design the switching signal.

Remark 6 In Algorithm 1, first of all, controller (2) is designed to guarantee that $\boldsymbol{A}_i + \boldsymbol{B}_i\boldsymbol{K}_i$ ($t \in T_{\mathrm{s}}[t_m, t_{m+1})$) is stable. Then, based on the stability of $\boldsymbol{A}_i + \boldsymbol{B}_i\boldsymbol{K}_j$ ($t \in T_{\mathrm{u}}[t_m, t_{m+1})$), the AED-ADT switching signal is designed. In ASIs, if all $\boldsymbol{A}_i + \boldsymbol{B}_i\boldsymbol{K}_j$ are stable, then only SAED-ADT is used; if all $\boldsymbol{A}_i + \boldsymbol{B}_i\boldsymbol{K}_j$ are unstable, then only FAED-ADT is adopted.

Algorithm 1 Design of controller gains and the switching signal

1: Set the values of λ_i, and solve inequality (22) to obtain $\bar{\boldsymbol{K}}_i$ and $\boldsymbol{X}_{i,i}$. Then we can obtain the controller gains $\boldsymbol{K}_i$ based on $\boldsymbol{K}_i = \bar{\boldsymbol{K}}_i \boldsymbol{X}_{i,i}^{-1}$.
2: Apply the values of $\boldsymbol{K}_i$ to determine whether $\boldsymbol{A}_i + \boldsymbol{B}_i\boldsymbol{K}_j$ is stable or unstable, and then confirm the ranges of the parameters $\gamma_{i,j}$ and $\mu_{i,j}$.
3: Set the values of $\nu_{i,j}$, $\gamma_{i,j}$, and $\mu_{i,j}$, and solve inequalities (23)–(25) to obtain $\boldsymbol{X}_{i,j}$ to verify the feasibility of solution $\boldsymbol{K}_i$. Then the corresponding AED-ADTs can be obtained.

In ASIs, when all $\boldsymbol{A}_i + \boldsymbol{B}_i\boldsymbol{K}_j$ are stable, we give the following corollary:

Corollary 1 Consider system (3). For the given values $\lambda_i < 0$ ($i \in \mathcal{M}$) with $\nu_{i,j} > 1$ ($(i,j) \in \Omega_{\mathrm{s}}$) and $\gamma_{i,j} < 0$ with $\mu_{i,j} > 1$ ($(i,j) \in \Omega_{\mathrm{u}\downarrow}$), if there exist matrices $\boldsymbol{X}_{i,i} > 0$ ($(i,i) \in \Omega_{\mathrm{s}}$), $\boldsymbol{X}_{i,j} > 0$ ($(i,j) \in \Omega_{\mathrm{u}\downarrow}$), and $\bar{\boldsymbol{K}}_i$ ($i \in \mathcal{M}$) such that inequalities (22)–(25) are true, then system (1) is stabilized under the asynchronous switching controller (2) and the switching signal that satisfies

$$\begin{cases} \tau_{i,j}^{\mathrm{a}} \geq \tau_{i,j}^{\mathrm{a}*} = -\dfrac{\ln \nu_{i,j}}{\lambda_i}, \ \ (i,j) \in \Omega_{\mathrm{s}}, \\ d_{i,j}^{\mathrm{a}} \geq d_{i,j}^{\mathrm{a}*} = -\dfrac{\ln \mu_{i,j}}{\gamma_{i,j}}, \ \ (i,j) \in \Omega_{\mathrm{u}\downarrow}. \end{cases}$$

Moreover, the controller gains are given by $\boldsymbol{K}_i = \bar{\boldsymbol{K}}_i \boldsymbol{X}_{i,i}^{-1}$.

In ASIs, when all $\boldsymbol{A}_i + \boldsymbol{B}_i\boldsymbol{K}_j$ are not stable, the following corollary can be obtained:

Corollary 2 Consider system (3). For the given values $\lambda_i < 0$ ($i \in \mathcal{M}$) with $\nu_{i,j} > 1$ ($(i,j) \in \Omega_{\mathrm{s}}$) and $\gamma_{i,j} > 0$ with $0 < \mu_{i,j} < 1$ ($(i,j) \in \Omega_{\mathrm{u}\uparrow}$), if there exist matrices $\boldsymbol{X}_{i,i} > 0$ ($(i,i) \in \Omega_{\mathrm{s}}$), $\boldsymbol{X}_{i,j} > 0$ ($(i,j) \in \Omega_{\mathrm{u}\uparrow}$), and $\bar{\boldsymbol{K}}_i$ ($i \in \mathcal{M}$) such that inequalities (22)–(25) are true, then system (1) is stabilized under the asynchronous switching controller (2) and the switching signal that satisfies

$$\begin{cases} \tau_{i,j}^{\mathrm{a}} \geq \tau_{i,j}^{\mathrm{a}*} = -\dfrac{\ln \nu_{i,j}}{\lambda_i}, \ \ (i,j) \in \Omega_{\mathrm{s}}, \\ d_{i,j}^{\mathrm{a}} \leq d_{i,j}^{\mathrm{a}*} = -\dfrac{\ln \mu_{i,j}}{\gamma_{i,j}}, \ \ (i,j) \in \Omega_{\mathrm{u}\uparrow}. \end{cases}$$

Moreover, the controller gains are given by $\boldsymbol{K}_i = \bar{\boldsymbol{K}}_i \boldsymbol{X}_{i,i}^{-1}$.

When $d(t) = 0$, that is, the switching between the system and the controller is synchronous, we have the following result:

Corollary 3 For any $(i,j) \in \mathcal{M} \times \mathcal{M}$, $i \neq j$, consider system (3). For the given scalars $\lambda_i < 0$ and $\nu_{i,j} > 1$, if there exist matrices $\boldsymbol{X}_{i,i} > 0$ and $\bar{\boldsymbol{K}}_i$ such that inequality (22) and the following inequality hold:

$$\boldsymbol{X}_j \leq \nu_{i,j}\boldsymbol{X}_i,$$

then system (1) is stabilized under controller $\boldsymbol{u}(t) = \boldsymbol{K}_{\sigma(t)}\boldsymbol{x}(t)$ and the switching signal that satisfies

$$\tau_{i,j}^{\mathrm{a}} \geq \tau_{i,j}^{\mathrm{a}*} = -\frac{\ln \nu_{i,j}}{\lambda_i}.$$

Moreover, the controller gains are given by $\boldsymbol{K}_i = \bar{\boldsymbol{K}}_i \boldsymbol{X}_{i,i}^{-1}$.

Proof The proof process is similar to that of Theorem 2, and thus it is omitted.

4 Examples

Now we provide two examples to show the effectiveness of the main results in this study.

Example 1 Consider the switched system (1) consisting of three subsystems. The parameters are as follows:

$$\boldsymbol{A}_1 = \begin{bmatrix} 2 & -0.2 \\ 0 & 2 \end{bmatrix}, \ \ \boldsymbol{A}_2 = \begin{bmatrix} -1 & 0 \\ 0 & 0.2 \end{bmatrix},$$

$$\boldsymbol{A}_3=\begin{bmatrix}-5 & 0\\ 0 & 2\end{bmatrix},\ \boldsymbol{B}_1=\begin{bmatrix}0.5 & 0\\ -0.1 & 0.2\end{bmatrix},$$
$$\boldsymbol{B}_2=\begin{bmatrix}0.4 & 0.1\\ 0 & 0.2\end{bmatrix},\ \boldsymbol{B}_3=\begin{bmatrix}-0.4 & 0.1\\ 0 & -0.2\end{bmatrix}.$$

The eigenvalues of matrix $\boldsymbol{A}_1$ are 2 and 2, those of matrix $\boldsymbol{A}_2$ are -1 and 0.2, and those of matrix $\boldsymbol{A}_3$ are -5 and 2, showing that these three subsystems are unstable. On the basis of Algorithm 1, we have the following steps:

Step 1: Let $\lambda_1=-1.2$, $\lambda_2=-3$, and $\lambda_3=-1$. Solving condition (22) in Theorem 2, we can obtain the values of $\boldsymbol{X}_{i,i}$ and $\bar{\boldsymbol{K}}_i$. By $\boldsymbol{K}_i=\bar{\boldsymbol{K}}_i\boldsymbol{X}_{i,i}^{-1}$, the controller gains can be obtained:

$$\boldsymbol{K}_1=\begin{bmatrix}-6.2000 & 0.3333\\ -2.9333 & -15.3333\end{bmatrix},$$
$$\boldsymbol{K}_2=\begin{bmatrix}-2.6429 & 2.4643\\ 0.5714 & -11.0000\end{bmatrix},$$
$$\boldsymbol{K}_3=\begin{bmatrix}-9.1667 & 2.0833\\ 3.3333 & 15.0000\end{bmatrix}.$$

Step 2: The eigenvalues of matrices $\boldsymbol{A}_{i,j}=\boldsymbol{A}_i+\boldsymbol{B}_i\boldsymbol{K}_j$ are illustrated in Table 1. The value ranges of the corresponding parameters $\mu_{i,j}$ and $\gamma_{i,j}$ are also presented in Table 1. From Table 1, we can see that only $\boldsymbol{A}_{2,1}=\boldsymbol{A}_2+\boldsymbol{B}_2\boldsymbol{K}_1$ is stable, and that the other $\boldsymbol{A}_{i,j}$ are unstable, which confirms that $\mu_{2,1}>1$, $\gamma_{2,1}<0$, and that the other $\mu_{i,j}$ and $\gamma_{i,j}$ $(i\neq j)$ satisfy $0<\mu_{i,j}<1$ and $\gamma_{i,j}>0$, respectively.

Table 1 Eigenvalues of matrices $\boldsymbol{A_{i,j}=A_i+B_iK_j}$

Matrix $\boldsymbol{A}_{i,j}$	eig($\boldsymbol{A}_{i,j}$)	$\mu_{i,j}$	$\gamma_{i,j}$
$\boldsymbol{A}_{1,2}$	0.0651, −2.2079	$0<\mu_{1,2}<1$	$\gamma_{1,2}>0$
$\boldsymbol{A}_{1,3}$	−1.6024, 5.9357	$0<\mu_{1,3}<1$	$\gamma_{1,3}>0$
$\boldsymbol{A}_{2,1}$	−5.4340, −2.9160	$\mu_{2,1}>1$	$\gamma_{2,1}<0$
$\boldsymbol{A}_{2,3}$	−3.6176, 4.4843	$0<\mu_{2,3}<1$	$\gamma_{2,3}>0$
$\boldsymbol{A}_{3,1}$	−1.9791, 5.7624	$0<\mu_{3,1}<1$	$\gamma_{3,1}>0$
$\boldsymbol{A}_{3,2}$	−2.9291, 5.2434	$0<\mu_{3,2}<1$	$\gamma_{3,2}>0$

Step 3: The parameters $\mu_{i,j}$, $\gamma_{i,j}$, and $\nu_{i,j}$, and the corresponding AED-ADTs are presented in Table 2.

From Table 2, we have the following conclusions:

1. In SSIs $[t_0,t_1)$ and $[t_m+d(t_m),t_{m+1})$, $m\in\mathbb{N}^+$, the ADTs $\tau_{i,j}$ are different based on different j, even for the same subsystem i. For example, $\tau_{1,2}^{\mathrm{a}}\geq\tau_{1,2}^{\mathrm{a}*}$ and $\tau_{1,3}^{\mathrm{a}}\geq\tau_{1,3}^{\mathrm{a}*}$ are both the dwell time on subsystem 1. We can see that they are not equal.

Table 2 Parameters $\boldsymbol{\nu_{i,j}}$, $\boldsymbol{\mu_{i,j}}$, $\boldsymbol{\gamma_{i,j}}$ and AED-ADTs $\boldsymbol{\tau_{i,j}^{a*}}$, $\boldsymbol{d_{i,j}^{a*}}$

$(i,\ j)$	$\nu_{i,j}$	$\mu_{i,j}$	$\gamma_{i,j}$	$\tau_{i,j}^{\mathrm{a}*}$	$d_{i,j}^{\mathrm{a}*}$
(1, 2)	1.7	0.6	8	0.4422	0.0639
(1, 3)	2.1	0.5	10	0.6183	0.0693
(2, 1)	1.2	2	−2	0.0608	0.3466
(2, 3)	1.3	0.8	9.5	0.0875	0.0235
(3, 1)	2.1	0.6	10	0.7409	0.0511
(3, 2)	2.1	0.5	9	0.7409	0.0770

2. In ASIs $[t_m,t_m+d(t_m))$, $m\in\mathbb{N}^+$, not only the ADTs on the same subsystem are different, but also the adopted switching signals may be different. For example, Table 1 shows that $\boldsymbol{A}_2+\boldsymbol{B}_2\boldsymbol{K}_1$ is stable but that $\boldsymbol{A}_2+\boldsymbol{B}_2\boldsymbol{K}_3$ is unstable for subsystem 2. That is, the controller $\boldsymbol{u}(t)=\boldsymbol{K}_1\boldsymbol{x}(t)$ can stabilize the second subsystem, but the controller $\boldsymbol{u}(t)=\boldsymbol{K}_3\boldsymbol{x}(t)$ cannot. In this case, in the intervals in which $\boldsymbol{A}_2+\boldsymbol{B}_2\boldsymbol{K}_1$ occurs, SAED-ADT switching is employed ($\mu_{2,1}=2>1$ and $\gamma_{2,1}=-2<0$ in Table 2). In cases in which $\boldsymbol{A}_2+\boldsymbol{B}_2\boldsymbol{K}_3$ is activated, the FAED-ADT switching works ($\mu_{2,3}=0.8<1$ and $\gamma_{2,3}=9.5>0$ in Table 2).

3. The ADTs in asynchronous switching are not necessarily smaller than the ones in SSIs, especially when $\boldsymbol{A}_i+\boldsymbol{B}_i\boldsymbol{K}_j$ is stable. For instance, Table 1 shows that $\boldsymbol{A}_2+\boldsymbol{B}_2\boldsymbol{K}_1$ is stable, and in Table 2, the corresponding ADT is $d_{2,1}^{\mathrm{a}}\geq d_{2,1}^{\mathrm{a}*}=0.3466$, which is larger than the ADT $\tau_{2,1}^{\mathrm{a}*}=0.0608$ in SSIs.

Choose the initial value $\boldsymbol{x}(0)=[2\ \ -4]^{\mathrm{T}}$ and the periodic switching path $1\to3\to2\to1\to3\to2\to\cdots$. Then, under the parameters in Table 2, Fig. 3a shows the response curves of state $\boldsymbol{x}(t)$ for the switching signal that satisfies condition (10) with $d_{3,1}^{\mathrm{a}}=0.01$, $\tau_{3,1}^{\mathrm{a}}=0.37$, $d_{2,3}^{\mathrm{a}}=0.06$, $\tau_{2,3}^{\mathrm{a}}=0.19$, $d_{1,2}^{\mathrm{a}}=0.06$, and $\tau_{1,2}^{\mathrm{a}}=0.24$. Fig. 3b presents the curves of these two signals. From Fig. 3, we can see that system (1) can be stabilized by the designed asynchronous switching controller (2) and switching signal (10). The response curve of the Lyapunov function $V(t)$ is shown in Fig. 4. From Fig. 4, we can see that on one hand the energy of $V(t)$ decreases in SSIs $[0,0.62)$, $[0.67,1.42)$, and $[1.44,1.53)$, but increases at the switching instants $t_1+d_{3,1}^{\mathrm{a}}=0.67$, $t_2+d_{2,3}^{\mathrm{a}}=1.44$, and $t_3+d_{1,2}^{\mathrm{a}}=1.59$. On the other

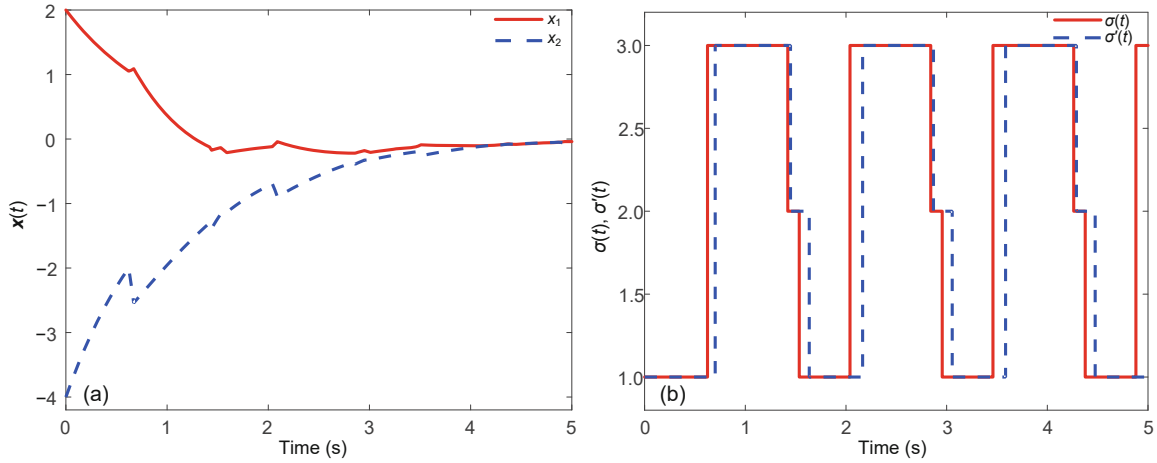

Fig. 3 Response curves of $x(t)$ (a) and switching signals $\sigma(t)$ and $\sigma'(t)$ (b) for Example 1

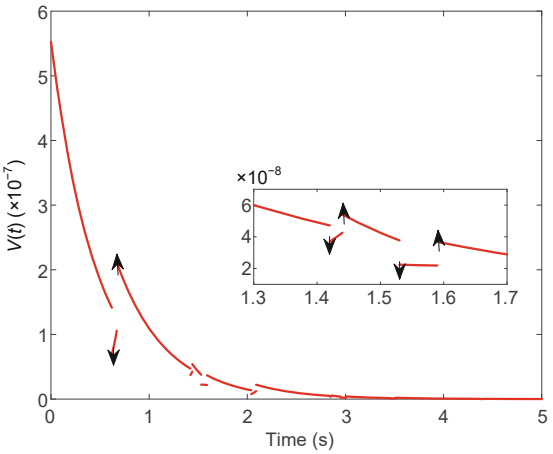

Fig. 4 Response curve of $V(t)$ for Example 1

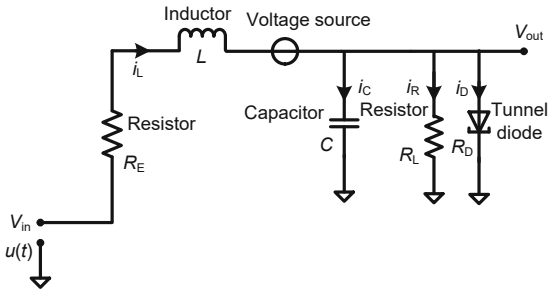

Fig. 5 Tunnel diode circuit

hand, at the switching instants $t_1 = 0.62$, $t_2 = 1.42$, and $t_3 = 1.53$, the energy of $V(t)$ is decreasing. Note that in ASIs $[0.62, 0.67)$ and $[1.42, 1.44)$, the energy increment of $V(t)$ is allowed.

Example 2 (Zhao et al., 2014) Consider the tunnel diode circuit presented in Fig. 5, which is described by

$$\begin{cases} C\dot{V}_{\rm C}(t) = -\frac{V_{\rm C}(t)}{R_{\rm L}} - \frac{1}{R_{\rm D}} + i_{\rm L}(t), \\ L\dot{i}_{\rm L}(t) = -V_{\rm C}(t) - R_{\rm E} i_{\rm L}(t) + 1.5V_{\rm C}(t) + u(t). \end{cases} \tag{27}$$

In practice, $R_{\rm D}$ is uncertain. Suppose $R_{\rm D} = 1/(0.002 + 0.01\beta)$, where $\beta \in [0, 100]$. Let $x_1(t) = V_{\rm C}(t)$ and $x_2(t) = i_{\rm L}(t)$. Then the above tunnel diode circuit can be described by the following equation:

$$\dot{\boldsymbol{x}}(t) = \boldsymbol{A}_{\sigma(t)}\boldsymbol{x}(t) + \boldsymbol{B}_{\sigma(t)}u(t),\ \sigma \in \{1,\ 2\},$$

with $\boldsymbol{x}(t) = [V_{\rm C},\ i_{\rm L}]^{\rm T}$ and

$$\boldsymbol{A}_1 = \begin{bmatrix} -\frac{1}{R_{\rm L}C} - \frac{1.002}{C} & \frac{1}{C} \\ \frac{1}{2L} & -\frac{R_{\rm E}}{L} \end{bmatrix},$$

$$\boldsymbol{A}_2 = \begin{bmatrix} -\frac{1}{R_{\rm L}C} - \frac{0.002}{C} & \frac{1}{C} \\ \frac{1}{2L} & -\frac{R_{\rm E}}{L} \end{bmatrix},$$

$$\boldsymbol{B}_1 = \boldsymbol{B}_2 = \begin{bmatrix} 0 \\ \frac{1}{L} \end{bmatrix}.$$

Here, the parameters are given by $C = 0.5$ F, $L = 0.01$ H, $R_{\rm E} = 0.1\ \Omega$, and $R_{\rm L} = 200\ \Omega$. Thus, we have

the following system matrices:

$$\boldsymbol{A}_1=\begin{bmatrix}-\dfrac{1007}{500} & 2\\ 50 & -10\end{bmatrix},\ \boldsymbol{A}_2=\begin{bmatrix}-\dfrac{7}{500} & 2\\ 50 & -10\end{bmatrix},$$
$$\boldsymbol{B}_1=\boldsymbol{B}_2=\begin{bmatrix}0\\ 100\end{bmatrix}.$$

Let $\lambda_1=-8$ and $\lambda_2=-5$. From inequality (22), we can obtain the values of controller gains $\boldsymbol{K}_i$ as

$$\boldsymbol{K}_1=[-0.5908\ 0.0245],$$
$$\boldsymbol{K}_2=[-0.6291\ 0.0311].$$

Then the eigenvalues of matrices $\boldsymbol{A}_{i,j}=\boldsymbol{A}_i+\boldsymbol{B}_i\boldsymbol{K}_j$ are illustrated in Table 3, showing that both matrices $\boldsymbol{A}_{1,2}$ and $\boldsymbol{A}_{2,1}$ are stable. Letting $\nu_{1,2}=2.5$, $\nu_{2,1}=3$, $\mu_{1,2}=2.5$, $\mu_{2,1}=3.5$, $\gamma_{1,2}=-5$, and $\gamma_{2,1}=-5$, we can obtain the corresponding AED-ADT as $\tau_{1,2}^{\mathrm{a}*}=0.1145$, $\tau_{2,1}^{\mathrm{a}*}=0.2197$, $d_{1,2}^{\mathrm{a}*}=0.1833$, and $d_{2,1}^{\mathrm{a}*}=0.2506$.

Table 3 Eigenvalues of matrices $\boldsymbol{A}_{i,j}=\boldsymbol{A}_i+\boldsymbol{B}_i\boldsymbol{K}_j$

Matrix $\boldsymbol{A}_{i,j}$	$\mathrm{eig}(\boldsymbol{A}_{i,j})$
$\boldsymbol{A}_{1,2}$	$-4.4535+4.4564\mathrm{i}$, $-4.4535-4.4564\mathrm{i}$
$\boldsymbol{A}_{2,1}$	$-3.7814+1.9932\mathrm{i}$, $-3.7814-1.9932\mathrm{i}$

Choose the initial value $\boldsymbol{x}(0)=[2\ \ -4]^{\mathrm{T}}$ and the periodic switching path $1\to2\to1\to2\to\cdots$. Fig. 6a shows the response curves of state $\boldsymbol{x}(t)$ for the switching signal that satisfies condition (10) with $\tau_{1,2}^{\mathrm{a}}=0.12$, $\tau_{2,1}^{\mathrm{a}}=0.22$, $d_{1,2}^{\mathrm{a}}=0.18$, and $d_{2,1}^{\mathrm{a}}=0.24$. Fig. 6b presents the curves of these two signals. From Fig. 6, we can determine that system (1) can be stabilized using the designed asynchronous switching controller (2) and switching signal (10). Fig. 7 presents the response curve of the Lyapunov function $V(t)$.

5 Conclusions

This study presents the research on the problem of stabilizing switched linear systems under asynchronous switching. SAED-ADT switching and FAED-ADT switching have been applied in designing the switching signal. Using the multi-Lyapunov function method, stabilization conditions have been given for switched linear systems. An algorithm has also been provided to determine the controller gains and to design the switching signals. Finally, two

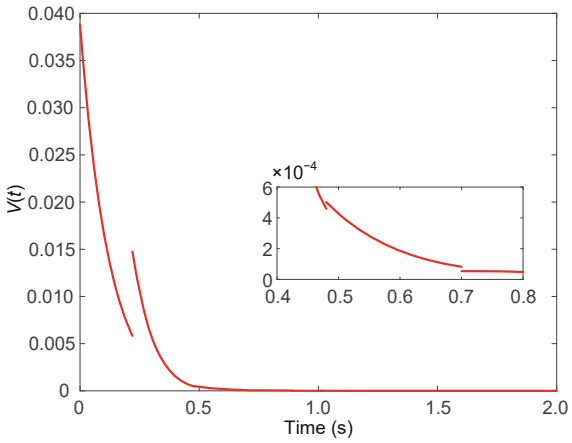

Fig. 7 Response curve of $V(t)$ for Example 2

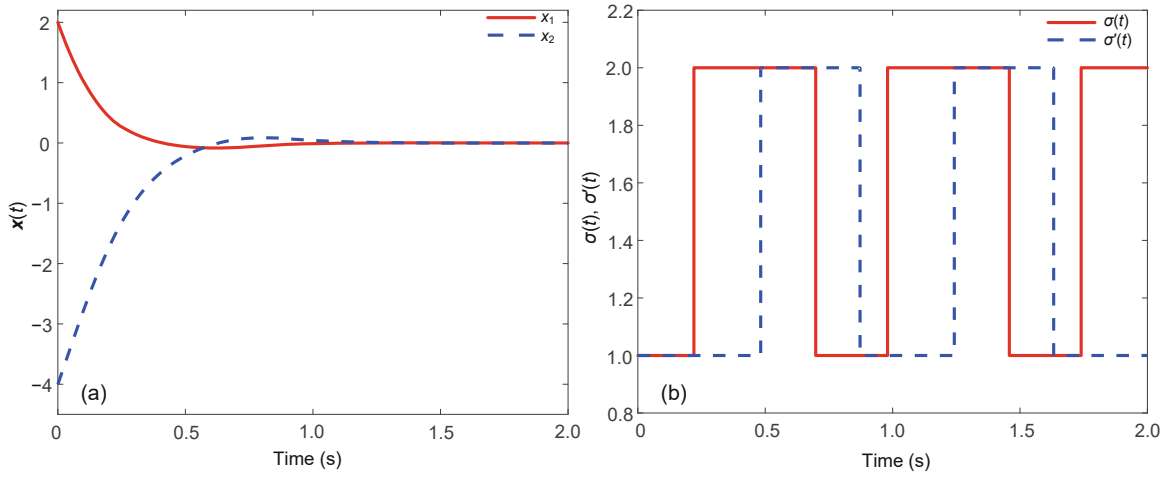

Fig. 6 Response curves of $\boldsymbol{x}(t)$ (a) and switching signals $\sigma(t)$ and $\sigma'(t)$ (b) for Example 2

examples have been given to show the effectiveness of the proposed results.

Note that in the practical automation industry, the occurrence of faults or failures in actuators and/or sensors will lead to degradation of system performance (Yang HY et al., 2018, 2021). In the future, we will study fault-tolerant control of switched linear systems under asynchronous switching and actuator failure.

Contributors

Linlin HOU designed the research. Linlin HOU and Xuan MA processed the data. Xuan MA carried out the simulations. Linlin HOU drafted the paper. Haibin SUN helped organize the paper. Xuan MA and Haibin SUN revised and finalized the paper.

Compliance with ethics guidelines

Linlin HOU, Xuan MA, and Haibin SUN declare that they have no conflict of interest.

References

Chang Y, Zhang S, Alotaibi ND, et al., 2020. Observer-based adaptive finite-time tracking control for a class of switched nonlinear systems with unmodeled dynamics. *IEEE Access*, 8:204782-204790. https://doi.org/10.1109/ACCESS.2020.3023726

Deaecto GS, Geromel JC, Daafouz J, 2011. Dynamic output feedback $H_{\inf}$ control of switched linear systems. *Automatica*, 47(8):1713-1720. https://doi.org/10.1016/j.automatica.2011.02.046

Deaecto GS, Souza M, Gernmel JC, 2015. Discrete-time switched linear systems state feedback design with application to networked control. *IEEE Trans Automat Contr*, 60(3):877-881. https://doi.org/10.1109/TAC.2014.2341131

Fei ZY, Shi S, Zhao C, et al., 2017. Asynchronous control for 2-D switched systems with mode-dependent average dwell time. *Automatica*, 79:198-206. https://doi.org/10.1016/j.automatica.2017.01.026

Fei ZY, Guan CX, Zhao XD, 2020. Event-triggered dynamic output feedback control for switched systems with frequent asynchronism. *IEEE Trans Automat Contr*, 65(7):3120-3127. https://doi.org/10.1109/TAC.2019.2945279

Hespanha JP, Morse AS, 1999. Stability of switched systems with average dwell-time. Proc 38$^{\text{th}}$ IEEE Conf on Decision Control, p.2655-2660. https://doi.org/10.1109/CDC.1999.831330

Hou LL, Zhao XD, Sun HB, et al., 2018a. l_2-l_∞ filtering of discrete-time switched systems via admissible edge-dependent switching signals. *Syst Contr Lett*, 113:17-26. https://doi.org/10.1016/j.sysconle.2017.10.005

Hou LL, Zhang MZ, Zhao XD, et al., 2018b. Stability of discrete-time switched systems with admissible edge-dependent switching signals. *Int J Syst Sci*, 49(5):974-983. https://doi.org/10.1080/00207721.2018.1439122

Hua CC, Liu GP, Zhang L, et al., 2019. Cooperative stabilization for linear switched systems with asynchronous switching. *IEEE Trans Syst Man Cybern Syst*, 49(6):1081-1087. https://doi.org/10.1109/TSMC.2017.2721644

Li ZM, Chang XH, Park JH, 2021. Quantized static output feedback fuzzy tracking control for discrete-time nonlinear networked systems with asynchronous event-triggered constraints. *IEEE Trans Syst Man Cybern Syst*, 51(6):3820-3831. https://doi.org/10.1109/TSMC.2019.2931530

Liberzon D, Morse AS, 1999. Basic problems in stability and design of switched systems. *IEEE Contr Syst*, 19(5):59-70. https://doi.org/10.1109/37.793443

Liu T, Wang C, 2019. Quasi-time-dependent asynchronous $\mathcal{H}_\infty$ control of discrete-time switched systems with mode-dependent persistent dwell-time. *Eur J Contr*, 48:66-73. https://doi.org/10.1016/j.ejcon.2018.11.002

Lu AY, Yang GH, 2020. Stabilization of switched systems with all modes unstable via periodical switching laws. *Automatica*, 122:109150. https://doi.org/10.1016/j.automatica.2020.109150

Ren HL, Zong GD, Li TS, 2018. Event-triggered finite-time control for networked switched linear systems with asynchronous switching. *IEEE Trans Syst Man Cybern Syst*, 48(11):1874-1884. https://doi.org/10.1109/TSMC.2017.2789186

Ren W, Xiong JL, 2016. Stability and stabilization of switched stochastic systems under asynchronous switching. *Syst Contr Lett*, 97:184-192. https://doi.org/10.1016/j.sysconle.2016.09.005

Sang H, Nie H, 2018. Asynchronous H_∞ control for discrete-time switched systems under state-dependent switching with dwell time constraint. *Nonl Anal Hybrid Syst*, 29:187-202. https://doi.org/10.1016/j.nahs.2018.01.007

Shi S, Shi ZP, Fei ZY, 2019. Asynchronous control for switched systems by using persistent dwell time modeling. *Syst Contr Lett*, 133:104523. https://doi.org/10.1016/j.sysconle.2019.104523

Shorten R, Wirth F, Mason O, et al., 2007. Stability criteria for switched and hybrid systems. *SIAM Rev*, 49(4):545-592. https://doi.org/10.1137/05063516X

Wang B, Zhang HB, Wang G, et al., 2014. Asynchronous control of discrete-time impulsive switched systems with mode-dependent average dwell time. *ISA Trans*, 53(2):367-372. https://doi.org/10.1016/j.isatra.2013.11.019

Wang XH, Zong GD, Sun HB, 2016. Asynchronous finite-time dynamic output feedback control for switched time-delay systems with non-linear disturbances. *IET Contr Theory Appl*, 10(10):1142-1150. https://doi.org/10.1049/iet-cta.2015.0577

Wang YE, Zhao J, Jiang B, 2013. Stabilization of a class of switched linear neutral systems under asynchronous switching. *IEEE Trans Automat Contr*, 58(8):2114-2119. https://doi.org/10.1109/TAC.2013.2250076

Wang YE, Wu BW, Wu CY, 2017. Stability and L_2-gain analysis of switched input delay systems with unstable modes under asynchronous switching. *J Franklin Inst*, 354(11):4481-4497. https://doi.org/10.1016/j.jfranklin.2017.04.006

Wang YQ, Xu N, Liu YJ, et al., 2021. Adaptive fault-tolerant control for switched nonlinear systems based

on command filter technique. *Appl Math Comput*, 392: 125725. https://doi.org/10.1016/j.amc.2020.125725

Wu YY, Cao JD, Li QB, et al., 2017. Finite-time synchronization of uncertain coupled switched neural networks under asynchronous switching. *Neur Netw*, 85:128-139. https://doi.org/10.1016/j.neunet.2016.10.007

Xiang WM, Xiao J, 2014. Stabilization of switched continuous-time systems with all modes unstable via dwell time switching. *Automatica*, 50(3):940-945. https://doi.org/10.1016/j.automatica.2013.12.028

Yang HY, Jiang YC, Yin S, 2018. Fault-tolerant control of time-delay Markov jump systems with *Itô* stochastic process and output disturbance based on sliding mode observer. *IEEE Trans Ind Inform*, 14(12):5299-5307. https://doi.org/10.1109/TII.2018.2812754

Yang HY, Jiang YC, Yin S, 2021. Adaptive fuzzy fault-tolerant control for Markov jump systems with additive and multiplicative actuator faults. *IEEE Trans Fuzzy Syst*, 29(4):772-785. https://doi.org/10.1109/TFUZZ.2020.2965884.

Yang JQ, Zhao XD, Bu XH, et al., 2018. Stabilization of switched linear systems via admissible edge-dependent switching signals. *Nonl Anal Hybrid Syst*, 29:100-109. https://doi.org/10.1016/j.nahs.2018.01.003

Yu Q, Zhai GS, 2021. A limit inferior Φ-dependent average dwell time approach for stability analysis of switched systems. *Int J Robust Nonl Contr*, 31(2):565-581. https://doi.org/10.1002/rnc.5291.

Yuan CZ, Wu F, 2015. Hybrid control for switched linear systems with average dwell time. *IEEE Trans Automat Contr*, 60(1):240-245. https://doi.org/10.1109/TAC.2014.2322941

Yuan S, Zhang LX, De Schutter B, et al., 2018. A novel Lyapunov function for a non-weighted L_2 gain of asynchronously switched linear systems. *Automatica*, 87:310-317. https://doi.org/10.1016/j.automatica.2017.10.018

Zhang LX, Gao HJ, 2010. Asynchronously switched control of switched linear systems with average dwell time. *Automatica*, 46(5):953-958. https://doi.org/10.1016/j.automatica.2010.02.021

Zhang XL, Lin AH, Zeng JP, 2014. Exponential stability of nonlinear impulsive switched systems with stable and unstable subsystems. *J Zhejiang Univ-Sci C (Comput & Electron)*, 15(1):31-42. https://doi.org/10.1631/jzus.C1300123

Zhao XD, Zhang LX, Shi P, et al., 2012. Stability and stabilization of switched linear systems with mode-dependent average dwell time. *IEEE Trans Automat Contr*, 57(7):1809-1815. https://doi.org/10.1109/TAC.2011.2178629

Zhao XD, Zhang LX, Shi P, et al., 2014. Robust control of continuous-time systems with state-dependent uncertainties and its application to electronic circuits. *IEEE Trans Ind Electron*, 61(8):4161-4170. https://doi.org/10.1109/TIE.2013.2286568

Zhao XD, Yin S, Li HY, et al., 2015. Switching stabilization for a class of slowly switched systems. *IEEE Trans Automat Contr*, 60(1):221-226. https://doi.org/10.1109/TAC.2014.2322961

Zhao XD, Yin YF, Zhang LX, et al., 2016. Control of switched nonlinear systems via T-S fuzzy modeling. *IEEE Trans Fuzzy Syst*, 24(1):235-241. https://doi.org/10.1109/TFUZZ.2015.2450834

Zhao XD, Kao YG, Niu B, et al., 2017. Control Synthesis of Switched Systems. Springer, Switzerland. https://doi.org/10.1007/978-3-319-44830-5